Phosphorus and boron codoping of silicon nanocrystals by ion implantation: Photoluminescence properties

Toshihiro Nakamura* and Sadao Adachi
Graduate School of Engineering, Gunma University, Kiryu, Gunma 376-8515, Japan

Minoru Fujii
Department of Electrical and Electronic Engineering, Graduate School of Engineering, Kobe University, Kobe 657-8501, Japan

Kenta Miura
Graduate School of Engineering, Gunma University, Kiryu, Gunma 376-8515, Japan

Shunya Yamamoto
Quantum Beam Science Directorate, Japan Atomic Energy Agency, Takasaki, Gunma 370-1292, Japan
(Received 8 September 2011; revised manuscript received 11 November 2011; published 25 January 2012)

The photoluminescence (PL) properties of P or B single-doped Si nanocrystals (Si-nc's) and P and B co-doped Si-nc's are studied. In the single-doped Si-nc samples, PL quenching occurs as a result of the Auger nonradiative recombination process between the photoexcited excitons and free carriers supplied by doped impurities. In the (P, B) co-doped sample, on the other hand, the donor-acceptor (D-A)-pair recombination emission is clearly observed on the long-wavelength side of the intrinsic Si-nc emission peak at ∼900 nm. The D-A-pair recombination energy is found to be smaller than the band-gap energy of bulk Si and is strongly dependent on the number of P and B impurities doped in a Si-nc. PL spectra are measured at 50 and 300 K and found to indicate that strong thermal quenching occurs in a (P, B) co-doped sample at 300 K. This quenching effect is probably because of carrier migration among the donor and acceptor states. The PL decay rate is determined as a function of the emitted-light wavelength for the pure and (P, B) co-doped Si-nc samples.

DOI: 10.1103/PhysRevB.85.045441 PACS number(s): 78.55.−m, 61.72.uf, 78.67.−n

I. INTRODUCTION

Si nanocrystals (Si-nc's) such as nanometer-sized Si dots embedded in a SiO_2 matrix[1,2] and porous Si (Refs. 3,4) have been intensively investigated because of their interesting photoluminescence (PL) properties. Si-nc's exhibit strong and visible emission at room temperature owing to the enhancement of the radiative recombination rate and band-gap widening resulting from carrier confinement in the nanostructured region.[5] Because of their compatibility with Si-based technology, light-emitting Si-nc's are an attractive candidate for materials used in various optoelectronic device applications.[6]

Impurity doping of a quantum-confined material system to control or improve its optical properties is an exciting challenge. Recently, it has been demonstrated that PL emission can be tuned by impurity doping (Cu and Mn) of colloidal ZnSe nc's.[7] In the study, the doped Cu and Mn states were observed to behave as emission centers. Moreover, efficient photoabsorption and subsequent transfer of the energy of the photoexcited carriers to the impurity states were observed in the colloidal ZnSe nc's.[7] InAs nc's heavily doped with a p-type impurity yielded a redshifted PL spectrum as a result of the formation of a quantum-confined impurity band and bandtailing.[8]

There have been some reports on impurity doping of Si-nc's to control their PL properties. By Er doping of Si-nc's embedded in a SiO_2 matrix, strong PL emission at ∼1.54 μm has been observed.[9,10] Co-doping of P and B as n- and p-type dopants in Si-nc's has also been studied, and PL emission with a peak below the band-gap energy of bulk Si crystal has been observed.[11] In the literature,[12] the PL peak energy and intensity are largely controlled by the P and B dopant concentrations.

It should be noted that in past studies, Si-nc's were deposited by rf sputtering.[11,12] Thus the size distribution of co-doped Si-nc's was thought to be different from that of undoped (pure) Si-nc's. Since the size of Si-nc's strongly affects their PL properties (PL peak energy, PL intensity, etc.), the difference of the size distribution between the co-doped and undoped Si-nc samples is a formidable barrier in the investigation of the effects of co-doping on the PL properties, e.g., in the determination of the donor-acceptor (D-A)-pair recombination energies in co-doped Si-nc's.

In this study, the PL properties of P and B co-doped Si-nc's are studied. (P, B) co-doping is performed by the ion implantation of rf-sputter-deposited Si-nc's embedded in a SiO_x matrix. Thus no change is expected in the size distribution of the Si-nc's after ion implantation. This is the main advantage of using the ion implantation technique. P and B single-doped samples are also prepared using the same technique. It is shown that (P, B) co-doping gives a new D-A-pair emission on the long-wavelength side of the intrinsic Si-nc emission peak. Quenching of the PL intensity is also observed in the P and B single-doped samples, and it is caused by the Auger nonradiative recombinaiton process between the photoexcited exciton and free carriers (*eeh* or *ehh* Auger process). The spectral dependence of the PL decay rates for the pure and (P, B) co-doped Si-nc samples is also examined.

II. EXPERIMENT

Pure Si-nc's embedded in glass matrices were prepared by the rf-sputtering method.[2] Small pieces of Si chips (5 × 15 mm^2) were placed on a SiO_2 sputtering target (10 cm in diameter). Thin films with a thickness of 700 nm were then deposited on fused silica glass in an Ar gas atmosphere. The concentration of excess Si in the deposited films was 4.81 wt %. After deposition, the films were annealed under N_2 gas flow at 1200 °C for 30 min. By this method, Si-nc's with an average diameter of 3.6 nm, estimated from the relationship between the PL peak wavelength and size,[2] were introduced in the SiO_2 matrices.

We prepared two types of samples, a P- or B-doped Si-nc and (P, B) co-doped Si-nc samples, by the ion implantation technique. For obtaining single-doped samples, P or B ions were implanted into Si-nc films by an ion implanter (Takasaki Ion Accelerators for Advanced Radiation Application of the Japan Atomic Energy Agency). The implantation energies of P and B ions were 250 and 100 keV, respectively. The ion doses of P and B were varied from 1 × 10^{14} to 4.5 × 10^{16} cm^{-2}. After implantation, rapid thermal annealing was performed by an image annealer (MILA-3000, ULVAC, Inc.) in N_2 gas flow at annealing temperatures (T_a) up to 1200 °C. The annealing time was 1 min.

In preparing (P, B) co-doped samples, P ions were first implanted in the Si-nc films and subsequently B ions were implanted. The implantation energies of P and B ions were 250 and 100 keV, respectively. The P ion dose was fixed at 4.5 × 10^{16} cm^{-2}, while the B ion dose was varied from 1 × 10^{14} to 4.5 × 10^{16} cm^{-2}. After implantation, rapid thermal annealing was performed in a N_2 atmosphere at temperatures up to 1200 °C. The annealing time was varied from 1 to 30 min. It should be noted that no strong PL emission was observed from samples annealed below 900 °C.

PL spectra of the P- or B-doped samples were measured at room temperature by a spectrometer (focal length: 15 cm; blaze wavelength: 500 nm; groove density: 150 g/mm) equipped with a charge-coupled device (Princeton Instruments, PIXIS 100B). The samples were excited by 325 nm radiation (spot size: ∼0.5 mm^2; power: 0.1 mW) from a He-Cd laser. We also used Ar ion (488.0 nm) and He-Ne (632.8 nm) lasers as excitation sources of the PL measurements and obtained essentially the same results as those reported in this paper (He-Cd laser). In the case of (P, B) co-doped samples, a spectrometer (focal length: 30 cm; blaze wavelength: 1090 nm; groove density: 150 g/mm) equipped with InGaAs photodiode array (Princeton Instruments, OMA V) was used as a photodetector. The (P, B) co-doped samples were excited by 405 nm light (spot size: ∼0.5 mm^2; power: 1 mW) from a laser diode. Time-resolved PL measurements were also performed on the (P, B) co-doped samples using a near-infrared photomultiplier tube (Hamamatsu R5509-72) and a multichannel scaler. PL and time-resolved PL measurements were performed at 50 and 300 K using a closed-cycle refrigerator cryostat. The spectral response of the PL detection system was corrected by using the reference spectrum of a standard tungsten lamp.

III. RESULTS AND DISCUSSION

A. P or B single-doped Si nanocrystal

Figure 1(a) shows PL spectra of P-implanted Si-nc's annealed at temperatures of 1000, 1100, and 1200 °C. The P ion dose was 4.5 × 10^{16} cm^{-2}. For comparison, the PL spectrum of pure Si-nc's is shown (the dashed curve). These spectra show the broad emission band with a peak at ∼800–900 nm. There have been reported several models, such as the quantum confined-exciton emission and silicon suboxides or interface states, which enable us to explain the PL emission mechanism from Si-nc's. In the present samples, the PL emission mechanism is to be mainly due to the quantum confined-exciton recombination in the Si-nc's. This is because of the clear size-dependent PL peak energies in the Si-nc's.[2] The PL intensity decreases with increasing T_a. Note that the pure Si-nc's showed no clear annealing temperature dependence of the PL properties from room temperature up to 1200 °C. One reason for the decrease in the PL intensity observed in Fig. 1(a) is the generation of internal and/or surface defects during P ion implantation. Although such defects can be considerably suppressed by postimplantation annealing,

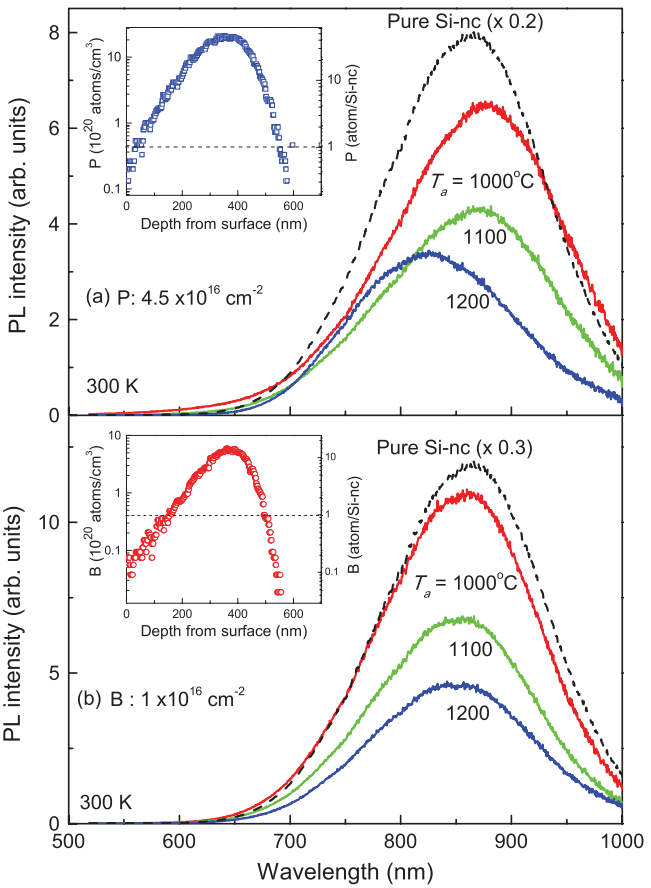

FIG. 1. (Color online) (a) PL spectra of pure (dashed curve) and P-implanted Si-nc's (solid curves) annealed at various temperatures (T_a). P ions were implanted at a dose of 4.5 ×10^{16} cm^{-2}. The annealing time was 1 min. The inset shows the calculated depth distribution of the P ions in SiO_2. The number of P atoms in a Si-nc is also shown on the right axis. (b) As (a), but for B-implanted (1 × 10^{16} cm^{-2}) Si-nc's.

their elimination is impossible. If the observed decrease in the PL intensity is mainly caused by the radiation-induced defects, then one can expect an increase in the PL intensity with increasing T_a. However, as shown in Fig. 1(a), what is observed is opposite to our expectation. Thus this reason can be ignored in the T_a range 1000–1200 °C.

There is another reason for the decrease in the PL intensity: the three-body Auger interaction between photoexcited excitons and the free electrons supplied by P doping.[13] Post-implantation annealing can remove radiation damages and move the implanted ion species into the Si lattice sites, resulting in an electrical activation of the implanted ions. Thus the probability of Auger nonradiative recombination process (*eeh* Auger process) may increase at higher post-implantation annealing temperatures, resulting in stronger quenching of the PL intensity. One can expect that at low doping concentration, no or weaker PL quenching should occur at higher annealing temperatures because of the weaker Auger nonradiative recombination process. In fact, the Si-nc samples implanted with P at the very low level of 4.5×10^{14} cm^{-2} showed the relatively strong PL intensity, twice stronger than that of highly implanted Si-nc sample (4.5×10^{16} cm^{-2}) annealed at 1200 °C. This fact further supports that the Auger nonradiative recombination process is the main reason for the PL quenching observed in the present study.

PL quenching resulting from the Auger process has been previously observed in P-doped Si-nc's prepared by co-sputtering methods.[13] The decrease in the PL intensity observed in the present study is about an order of magnitude, which is smaller than that observed in the co-sputtered samples (a decrease of about two orders of magnitude).[12] This is probably because of the inhomogeneous distribution of the implanted P ions. The inset of Fig. 1(a) shows the depth distribution of the implanted P ions in the film layer, calculated by TRIM.[14] The peak of the depth distribution is located around the center of the film layer (∼360 nm in depth from the sample surface). After annealing, the implanted P atoms can diffuse deep into the film layer. However, the annealing time is very short (1 min) and the diffusion constant of P in SiO_2 is much smaller than that in Si (3.3×10^{-16} cm^2/s in SiO_2 and 1.2×10^{-12} cm^2/s in Si at 1200 °C).[15,16] One can therefore expect the distribution of P to be almost unchanged after annealing. As shown in the inset of Fig. 1(a), the concentrations of P atoms at the surface and deep in the film region are much lower than that at the center of the film layer. The density of sufficiently P-doped Si-nc's at the surface and deep in the film is low, resulting in the weak quenching of the PL intensity as a consequence of the Auger recombination process (*eeh*).

In Fig. 1(b), PL spectra of B-implanted Si-nc's annealed at various temperatures are shown. The B ion dose was 1×10^{16} cm^{-2}. Similar to the P-implanted Si-nc's, the PL intensity of the B-implanted Si-nc's decreased with increasing annealing temperature. This decrease is also thought to be due to the Auger nonradiative recombination process[17] together with the nonradiative recombination at the surface and/or internal defects introduced in the Si-nc's by ion implantation. In the inset of Fig. 1(b), the calculated depth distribution of the implanted B ions is shown. The distribution is inhomogeneous and its width is slightly smaller than that of P ions.

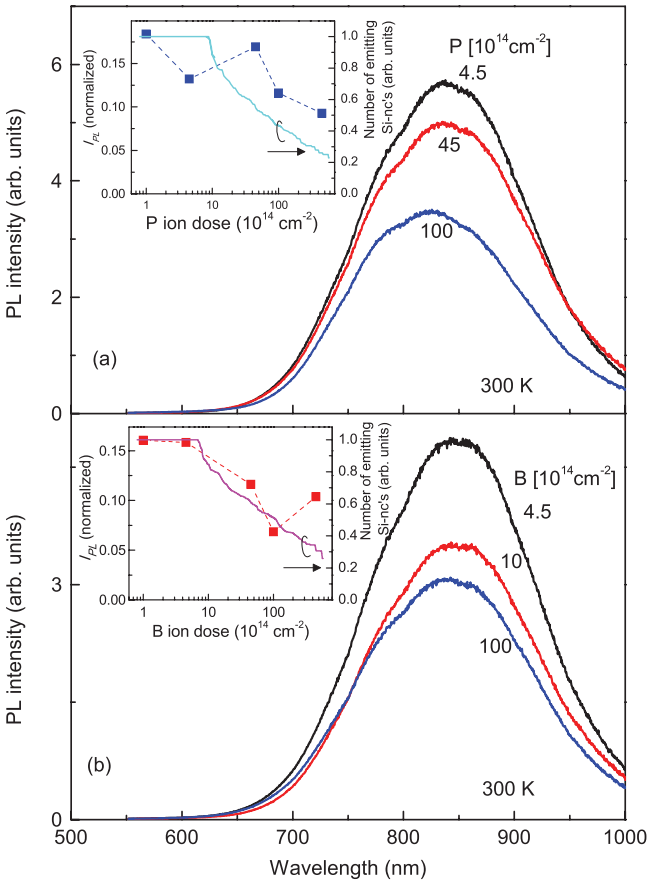

FIG. 2. (Color online) (a) PL spectra of P-implanted Si-nc's for various ion doses and after annealing at a T_a of 1200 °C. The annealing time was 1 min. The inset shows I_{PL} for P-implanted Si-nc's (normalized by that of pure Si-nc's) as a function of the P ion dose (solid squares). The number of light-emitting Si-nc's calculated from the distribution of P atoms in the inset of Fig. 1(a) is also shown (solid curve, right axis). (b) As (a), but for B-implanted Si-nc's.

Figure 2(a) shows the PL spectra of Si-nc's implanted with P ions at various doses and annealed at a T_a of 1200 °C. The PL intensity decreases with increasing P ion dose. The integrated PL intensity I_{PL} is plotted as a function of the P ion dose in the inset of Fig. 2(a). The value of I_{PL} is normalized by that for pure Si-nc's. Although the data are scattered, I_{PL} decreases above 1×10^{16} cm^{-2}. In Fig. 2(b), the PL spectra of B-ion-implanted Si-nc's annealed at a T_a of 1200 °C are shown for various ion doses. The inset of Fig. 2(b) shows plots of I_{PL} versus B ion dose. A monotonous decrease in the PL intensity is observed in the higher B ion dose region, except for the highest ion dose (4.5×10^{16} cm^{-2}).

To obtain more quantitative information on the dependence of I_{PL} on the P and B ion doses, we estimate the number of light-emitting Si-nc's, which is assumed to be proportional to the observed PL intensity, under a simple assumption. Because of the inhomogeneous distribution of the implanted P or B ions (Fig. 1), the number of P- or B-doped Si-nc's is strongly dependent on the depth of the Si-nc film. Under the assumption that Si-nc's are uniformly distributed in the film layer and they have a spherical shape with a diameter of 3.6 nm, the numbers of P and B atoms in a Si-nc can be calculated from

the depth distributions of the atoms. In the insets of Fig. 1, the calculated number of P or B atoms per Si-nc is shown as a function of the film depth on the right axis. Each Si-nc near the center of the film layer contains more than one P or B atom, while at or near the surface and far from the surface, the number of P or B atoms is lower than unity. Assuming that Si-nc's containing more than one P or B atom do not emit light because of the Auger nonradiative recombination process, the number of light-emitting Si-nc's can be calculated from the depth profile of P or B ions in the film.

In the insets of Fig. 2, the calculated numbers of light-emitting Si-nc's are shown as a function of (a) P and (b) B ion doses (solid curves, right axes). For both P and B ions, the number of light-emitting Si-nc's steeply decreases at around 1×10^{15} cm^{-2} and then gradually decreases with a further increase in the ion dose. For P-doped Si-nc's [the inset of Fig. 2(a)], the dose dependence of I_{PL} is different from that of the number of light-emitting Si-nc's (I_{PL} decreases above $\sim 1 \times 10^{16}$ cm^{-2}, while the number of light-emitting Si-nc's decreases above $\sim 1 \times 10^{15}$ cm^{-2}). On the other hand, for B-doped Si-nc's [the inset of Fig. 2(b)], the experimentally determined dose dependence of I_{PL} roughly follows the number of light-emitting Si-nc's. This result for the B-doped Si-nc's indicates the suggestion that the main reason for the PL quenching is the Auger nonradiative recombination process. We must note, however, that the Auger recombination is a complex statistical process that depends on the available electrons and holes, as well as available empty states for the excited electrons or holes. This may be a cause for the disagreement between the calculation and experiment in the inset of Fig. 2(a).

In the case of P-doped Si-nc's, there are two possible reasons for the difference between the dose dependence of I_{PL} and that of the number of light-emitting Si-nc's. One is the surface passivation effect of P atoms.[13,18] The passivation of Si-nc surfaces by P atoms at the Si/SiO_2 interface leads to an increase in the number of efficient light-emitting Si-nc's (i.e., an increase in the PL intensity) with increasing P dose. This dose dependence is in contrast to that expected in the case of the Auger nonradiative recombination process. Therefore the passivation by P atoms may mask the presently observed PL quenching phenomenon. Another reason is the increase in the radiative recombination rate associated with P impurity doping.[19–21] This effect can also lead to an increase in the PL intensity with increasing P concentration. A more detailed study is needed to confirm this possibility.

B. (P, B) co-doped Si nanocrystal

In Fig. 3(a), PL spectra of (P, B) co-doped Si-nc's annealed at 1000, 1100, and 1200 °C are shown. Both P and B ions were implanted at a dose of 4.5×10^{16} cm^{-2}. The annealing time was 1 min. The spectrum of pure Si-nc is also shown in Fig. 1(a). The PL spectral shape and intensity are strongly dependent on T_a. For example, the PL spectrum broadens in the long-wavelength region with increasing T_a. As a result, for samples annealed at 1100 and 1200 °C, the emission band tails penetrate well below the band-gap energy of the bulk Si crystal (1.12 eV; horizontal dashed line). Furthermore, the PL intensity increases with T_a.

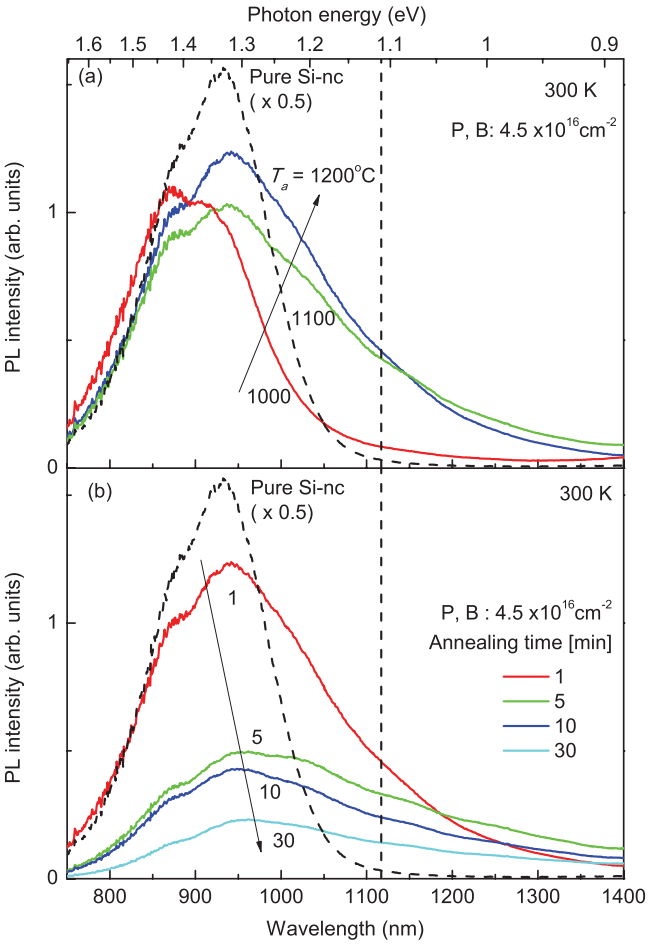

FIG. 3. (Color online) (a) PL spectra of pure (dashed curve) and (P, B) co-doped Si-nc's (solid curves) annealed at various temperatures. Each P and B ion dose was implanted at a dose of 4.5×10^{16} cm^{-2}. The annealing time was 1 min. (b) PL spectra of pure (dashed curve) and (P, B) co-doped Si-nc's (solid curves) annealed at 1200 °C for various annealing times. P and B ions were implanted at a dose of 4.5×10^{16} cm^{-2}.

The dependence of the spectral broadening and PL intensity on the annealing temperature for the co-doped sample is quite different from that for the P or B single-doped sample (Fig. 1). The spectral broadening and the increase in the PL intensity in the (P, B) co-doped samples annealed at high temperatures are attributed to the effect of carrier compensation and photoexcited electron-hole-pair recombination in the donor and acceptor states.[11,12] Upon co-doping with P and B, the donor and acceptor states are introduced in the forbidden gap of Si-nc's. Optically excited carriers can then recombine in the donor and acceptor states and emit light in the sub-band-gap spectral region. Upon annealing at a higher temperature, a larger number of implanted ions are activated, resulting in an increase in the PL intensity.

Figure 3(b) shows PL spectra of (P, B) co-doped Si-nc's isothermally annealed from 1 to 30 min at 1200 °C. The P and B doses were 4.5×10^{16} cm^{-2}. It is found that the PL intensity decreases with increasing annealing time. The decrease in the PL intensity is probably due to the broader impurity distribution that results from annealing for a longer

time. To observe D-A-pair emission, it is necessary that both the donor and acceptor states be activated in the Si-nc's. Since the diffusion coefficients of P and B in SiO_2 are different (3.3×10^{-16} cm^2/s and 1.1×10^{-16} cm^2/s, respectively),[15] the difference between the concentration distribution of P and that of B increases with the annealing time. As a result, the number of (P, B) co-doped Si-nc's decreases, and thus the PL intensity decreases with increasing annealing time. Furthermore, the PL band tail slightly extends toward the longer-wavelength side with increasing annealing time. This tailing can also be explained by the larger deviation in the P and B concentration profiles upon annealing for a longer time.

The B ion dose dependence of the PL spectra of (P, B) co-doped Si-nc's is shown in Fig. 4(a). The P ion dose was fixed at 4.5×10^{16} cm^{-2}. At lower B ion doses (less than about 1×10^{15} cm^{-2}), the observed PL intensities are very weak. With increasing B ion dose, the PL intensity becomes stronger, and simultaneously, the band tailing toward the longer-wavelength side becomes remarkable. These observations also provide clear evidence of carrier compensation and D-A-pair recombination in the co-doped Si-nc's. In the case of lower B ion doses, because the most Si-nc's are doped mainly with P, Auger nonradiative recombination may be dominant. At higher B ion doses, on the other hand, the most Si-nc's contain both P and B, which leads to the recovery of the ordinary PL emission peak at ~900 nm and simultaneously produces the D-A-pair recombination peak.

It is interesting to note that in Fig. 4(a), while the high-energy cutoff (1.63 eV; bold vertical arrow) in all PL spectra is almost the same, the low-energy cutoff is clearly dependent on the B ion dose (light vertical arrows). For pure Si-nc's, the PL spectral width is determined not only from the size distribution of Si-nc's,[5,22] but also from an intrinsic homogeneous broadening, which is temperature dependent. Thus the high- and low-energy cutoffs can represent the band-gap energies of the smallest and largest Si-nc's, E_{gh}^{pure} and E_{gl}^{pure}. In (P, B) co-doped samples, the nanocrystal size distribution is not changed after ion implantation. Therefore the low-energy cutoff in the (P, B) co-doped samples represents the energy difference E_{gl}^{codope} between the lowest donor and highest acceptor states. In the inset of Fig. 4(a), a sketch of the energy differences E_{gh}^{pure}, E_{gl}^{pure}, and E_{gl}^{codope} in (P, B) co-doped Si-nc's is shown.

The values of E_{gh}^{pure}, E_{gl}^{pure}, and E_{gl}^{codope} are shown as a function of the B ion dose in Fig. 4(b). As expected, E_{gh}^{pure} is nearly constant regardless of the B ion dose. In contrast, E_{gl}^{codope} clearly decreases with an increase in the B ion dose. Note that E_{gl}^{codope} is always smaller than the band-gap energy of bulk Si (1.12 eV). From the data in Fig. 4(b), the D-A-pair energy shift (resulting from impurity doping) with respect to the band-gap energy of pure Si-nc's can be obtained. Let us define a change in the D-A-pair emission energy by $\Delta_{\text{min}} = E_{gl}^{\text{pure}} - E_{gl}^{\text{codope}}$. In the inset of Fig. 4(b), Δ_{min} is plotted as a function of the B ion dose. The upper horizontal axis shows the number of B atoms in a Si-nc. Δ_{min} rapidly increases when the number of B atoms is small (~1 atom/Si-nc). For the maximum number of B atoms (~70 atoms/Si-nc), the value of Δ_{min} is 230 meV. This result indicates that when

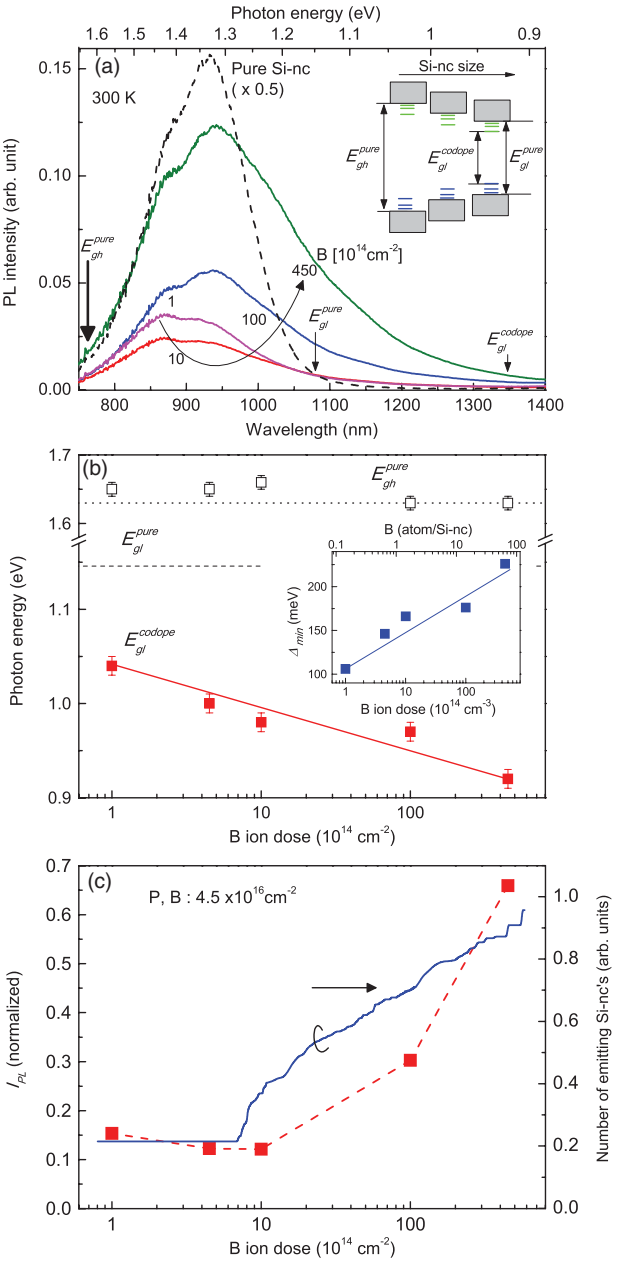

FIG. 4. (Color online) (a) PL spectra of pure (dashed curve) and (P, B) co-doped Si-nc's (solid curves) annealed at 1200 °C. The P ion dose was 4.5×10^{16} cm^{-2}. The B ion dose was varied from 1×10^{14} to 4.5×10^{16} cm^{-2}. The annealing time was 1 min. (b) E_{gh}^{pure}, E_{gl}^{pure}, and E_{gl}^{codope} as a function of the B ion dose. The inset shows Δ_{min} as a function of the B ion dose (lower horizontal axis) and the number of B ions in the Si-nc (upper horizontal axis). (c) I_{PL} for the (P, B) co-doped Si-nc's (normalized by that of pure Si-nc's) as a function of the B ion dose (solid squares, left axis). The number of light-emitting Si-nc's calculated from the distributions of the B and P atoms is also shown (solid curve, right axis).

the number of dopant atoms (B) is small, it significantly affects the energy levels of impurity states. The similar results have previously been obtained for heavily doped InAs nc's.[8]

In Fig. 4(c), I_{PL} is shown as a function of the B ion dose for (P, B) co-doped samples (solid squares). I_{PL} is normalized

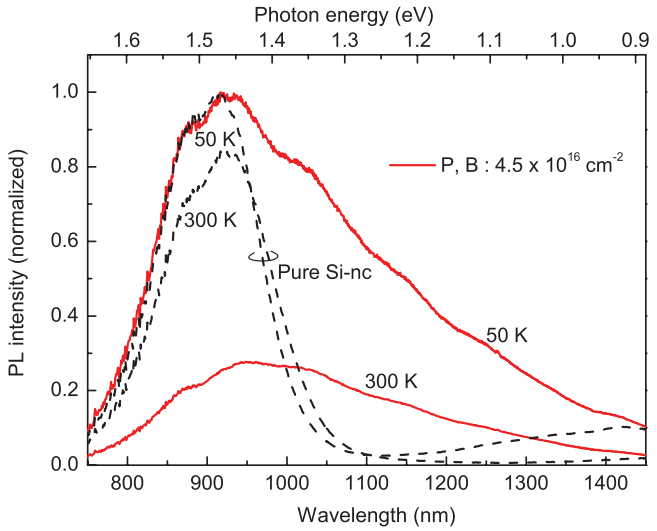

FIG. 5. (Color online) Room- (300 K) and low-temperature (50 K) PL spectra of pure (dashed curves) and (P, B) co-doped Si-nc's (solid curves) annealed at 1200 °C. The P and B ion doses were 4.5 $\times$ 10^{16} cm^{-2}. The annealing time was 1 min.

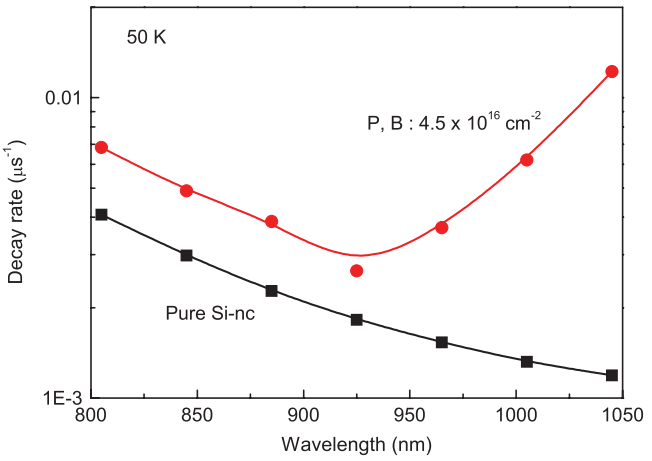

FIG. 6. (Color online) Emitted-light wavelength dependence of the PL decay rate for pure (solid squares) and (P, B) co-doped Si-nc (solid circles) samples at 50 K. The P and B ion doses were 4.5 $\times$ 10^{16} cm^{-2}.

by the I_{PL} value for pure Si-nc's. The recovery of the PL intensity is observed at higher B ion doses. At the highest B ion dose, the value of I_{PL} is about 0.7. To explain the B dose dependence of I_{PL}, we calculate the number of light-emitting Si-nc's using a procedure similar to that used before. Here, the light-emitting Si-nc's are regarded as a mixture of co-doped and undoped Si-nc's.

The result of this calculation is shown in Fig. 4(c). The number of Si-nc's exhibiting D-A-pair emission is determined mainly from the B concentration profile. Thus both the integrated PL intensity I_{PL} and the number of light-emitting Si-nc's exhibit similar dependence on the B ion dose, as shown in Fig. 4(c). Note that the relative value (∼0.2–0.3) of the number of light-emitting Si-nc's in the lower B ion region is more representative of the intrinsic Si-nc's, which can also emit light in the ∼750–1050-nm region [see Fig. 4(a)].

Next, we discuss the temperature dependence of the PL properties of co-doped Si-nc's. In Fig. 5, PL spectra of (P, B) co-doped and pure Si-nc's measured at 50 and 300 K are shown. The P and B ions were implanted at a dose of 4.5 $\times$ 10^{16} cm^{-2}. Each spectrum was normalized by the 50-K peak intensity. For the co-doped sample, strong thermal quenching is observed at 300 K. Interestingly, no such strong thermal quenching was observed for the pure Si-nc sample. Moreover, a weak emission band is clearly observed at ∼1400 nm (0.9 eV) in the pure Si-nc sample at 50 K, and it can be attributed to the recombination of carriers trapped in the surface defect states of the Si-nc.[23] Thermal quenching has also been observed in (P, B) co-doped Si-nc's prepared by the co-sputtering method.[11]

We note that the degree of thermal quenching in the co-doped Si-nc sample by ion implantation is larger than that doped by the co-sputtering method.[11] This may be because of the higher donor and acceptor concentrations in the ion-implanted sample. Assuming that only a single donor-acceptor pair exists in a Si-nc, no strong thermal quenching can be expected.[11] When a large number of donors and acceptors are introduced, nonradiative recombination of the excited carriers occurs as a result of thermalization and migration among the donor and acceptor states. In the co-sputtered sample, the average number of donor and acceptor pairs in a Si-nc is ∼1,[11] which ensures the absence of strong thermal quenching. In contrast, the number of donor-acceptor pairs in the (P, B) co-implanted sample is strongly dependent on the film depth, and its maximum value is estimated to be about 50. Therefore strong thermal quenching can be expected in the (P, B) co-implanted sample.

Finally, in Fig. 6 we show the PL decay rate, which was obtained from time-resolved PL measurements at 50 K, as a function of the emitted-light wavelength for pure and (P, B) co-doped Si-nc's. For pure Si-nc's, the PL decay rate decreases with increasing emitted-light wavelength. This can be understood by considering an enhancement in the radiative recombination rate as a consequence of the quantum-confinement effect.[24] The decay rates for the co-doped Si-nc's are observed to be larger than those for the pure Si-nc's, over the entire wavelength range investigated. Moreover, the decay rate for the co-doped Si-nc's increases at wavelengths above 950 nm. Note that the PL emission due to the D-A-pair recombination is observed on the long-wavelength side. Therefore the observed wavelength dependence of the decay rate in Fig. 6 indicates that the D-A-pair recombination process has a larger radiative decay rate than that of the intrinsic exciton recombination process in pure Si-nc's.

The decay rate can be principally written as $W = W_r + W_{nr}$, where W_r and W_{nr} are, respectively, the radiative and nonradiative decay rates. The larger decay rates in the intrinsic emission region (<950 nm) in the (P, B) co-doped Si-nc's, compared to those of the pure Si-nc's, in Fig. 6 are thought to be associated with the nonradiative term W_{nr}, and to be caused by implantation-induced crystalline damage. The larger decay rates observed in the D-A-pair emission region ($\geqslant$950 nm) can also be a result of the effect of the defect-trapped nonradiative recombination process.

IV. CONCLUSIONS

The PL properties of (P, B) co-doped Si-nc's were studied. The *n*- and *p*-type dopants P and B were implanted in pure Si-nc films prepared by the rf-sputtering method. For a P or B single-doped sample, the quenching of the PL intensity due to Auger nonradiative recombination process (*eeh* or *ehh*) between the photoexcited excitons and carriers supplied by implanted dopants was observed. For (P, B) co-doped Si-nc's, the D-A-pair recombination emission was clearly observed on the long-wavelength side of the intrinsic Si-nc emission peak at ∼900 nm. From our measured PL spectra of co-doped Si-nc's, we determined the exact D-A-pair emission energies. This led to findings that the D-A-pair recombination energies are observed to be smaller than the band-gap energy of bulk Si (∼1.12 eV) and are strongly dependent on the number of P and B impurity atoms in the Si-nc. Strong temperature dependence of the PL intensity was observed in the (P, B) co-doped sample, and it was considered to be because of the carrier migration among the donor and acceptor states. The spectral dependence of the PL decay rates in the pure and (P, B) co-doped Si-nc samples was determined and discussed. Because the co-doped Si-nc samples with P/B showed the broad PL emission band largely extending from the visible to the near-infrared region, it may be possible to use such Si-nc materials as an active medium in a variety of Si photonics (e.g., tunable light emitters/detectors in the 0.8–1.0-μm wavelength region).

ACKNOWLEDGMENTS

This work was partly supported by Grants-in-Aid for Young Scientists (B) (Grant No. 22760050) and Scientific Research (B) (Grant No. 23360133) from the Ministry of Education, Culture, Sports, Science and Technology, Japan. We would like to thank O. Hanaizumi, T. Miyazaki, H. Oike, and M. Nojiri for their support with the experiments.

*nakamura@el.gunma-u.ac.jp

[1] K. S. Min, K. V. Shcheglov, C. M. Yang, H. A. Atwater, M. L. Brongersma, and A. Polman, Appl. Phys. Lett. **69**, 2033 (1996).
[2] S. Takeoka, M. Fujii, and S. Hayashi, Phys. Rev. B **62**, 16820 (2000).
[3] L. T. Canham, Appl. Phys. Lett. **57**, 1046 (1990).
[4] A. G. Cullis, L. T. Canham, and D. J. Calcott, J. Appl. Phys. **82**, 909 (1997).
[5] D. Kovalev, H. Heckler, G. Polisski, and F. Koch, Phys. Status Solidi B **215**, 871 (1999).
[6] L. Pavesi, L. D. Negro, C. Mazzoleni, G. Franzo, and F. Priolo, Nature (London) **408**, 440 (2000).
[7] N. Pradhan, D. Goorskey, J. Thessing, and X. Peng, J. Am. Chem. Soc. **127**, 17586 (2005).
[8] D. Mocatta, G. Cohen, J. Schattner, O. Millo, E. Rabani, and U. Banin, Science **332**, 77 (2011).
[9] A. J. Kenyon, P. F. Trwoga, M. Federighi, and C. W. Pitt, J. Phys.: Condens. Matter **6**, L319 (1994).
[10] M. Fujii, M. Yoshida, Y. Kanzawa, S. Hayashi, and K. Yamamoto, Appl. Phys. Lett. **71**, 1198 (1997).
[11] M. Fujii, K. Toshikiyo, Y. Takase, Y. Yamaguchi, and S. Hayashi, J. Appl. Phys. **94**, 1990 (2003).
[12] M. Fujii, Y. Yamaguchi, Y. Takase, K. Ninomiya, and S. Hayashi, Appl. Phys. Lett. **85**, 1158 (2004).
[13] A. Mimura, M. Fujii, S. Hayashi, D. Kovalev, and F. Koch, Phys. Rev. B **62**, 12625 (2000).
[14] J. Biersack and L. Haggmark, Nucl. Instrum. Methods **174**, 257 (1980).
[15] T. Aoyama, H. Tashiro, and K. Suzuki, J. Electrochem. Soc. **146**, 1879 (1999).
[16] H. G. Francois-Saint-Cyr, F. A. Stevie, J. M. McKinley, K. Elshot, L. Chow, and K. A. Richardson, J. Appl. Phys. **94**, 7433 (2003).
[17] A. Mimura, M. Fujii, S. Hayashi, and K. Yamamoto, Solid State Commun. **109**, 561 (1999).
[18] A. L. Tchebotareva, M. J. A. de Dood, J. S. Biteen, H. A. Atwater, and A. Polman, J. Lumin. **114**, 137 (2005).
[19] A. N. Mikhaylov, D. I. Tetelbaum, V. A. Burdov, O. N. Gorshkov, A. I. Belov, D. A. Kambarov, V. A. Belyakov, V. K. Vasiliev, A. I. Kovalev, and D. M. Gaponova, J. Nanosci. Nanotechnol. **8**, 780 (2008).
[20] V. A. Belyakov and V. A. Burdov, Phys. Rev. B **79**, 035302 (2009).
[21] K. Murakami, R. Shirakawa, M. Tsujimura, N. Uchida, N. Fukata, and S. Hishita, J. Appl. Phys. **105**, 054307 (2009).
[22] G. Ledoux, O. Guillois, D. Porterat, C. Reynaud, F. Huisken, B. Kohn, and V. Paillard, Phys. Rev. B **62**, 15942 (2000).
[23] B. K. Meyer, D. M. Hofmann, W. Stadler, V. Petrova-Koch, F. Koch, P. Omling, and P. Emanuelsson, Appl. Phys. Lett. **63**, 2120 (1993).
[24] M. S. Hybertsen, Phys. Rev. Lett. **72**, 1514 (1994).